ZIBELINE INTERNATIONAL™ PUBLISHING

ISSN: 2521-5035 (Print)
ISSN: 2521-5043 (Online)
CODEN: ESMACU

Earth Sciences Malaysia (ESMY)

DOI: http://doi.org/10.26480/esmy.01.2023.36.42

CrossMark

RESEARCH ARTICLE

MODELLING URBAN SPRAWL OF THE GREATER PORT HARCOURT CITY USING REMOTE SENSING AND GEOGRAPHIC INFORMATION SYSTEM TECHNIQUES

Chukwubueze Onwuzuligbo[a], Uzoma Chinenye Okeke[a], Onah Emmanuel Udochukwu[b], Iyam Ubi Effiom[c], John-Uri Kikpoye[d]

[a] Department of Surveying and Geoinformatics, Nnamdi Azikiwe University, Awka, Nigeria.
[b] Department of Geoinformatics and Surveying, University of Nigeria, Enugu Campus.
[c] Office of the Surveyor General, Calabar, Cross River State, Nigeria
[d] Greater Port Harcourt city Development Authority, km 33 Port Harcourt, Nigeria.
**Corresponding Author Email: cu.onwuzuligbo@unizik.edu.ng*

ARTICLE DETAILS

Article History:

Received 10 September 2022
Revised 22 October 2022
Accepted 28 November 2022
Available online 30 November 2022

ABSTRACT

In recent decades, urban sprawl has been viewed as one of the most pressing issues that cities over all the world in developing countries are batting with. It is often associated mostly with rural-urban migration and rising birth rates, where development is given precedence over urban planning. The study focuses on the urban sprawl of the greater Port Harcourt city. The greater Port Harcourt city is expanding at an unprecedented rate, with no adequate planning or statistical record. The study intends to address this issue by building models using remote sensing and geographic information system (GIS) tools in order to analyze urban sprawl in the Greater Port Harcourt city. To achieve this set of objectives, three sets of Landsat sensors, which were captured at different time intervals (1986, 2006, and 2021), were used to monitor urban sprawl in the study area. The Geographic Positioning System (GPS) was used during the field visit to collect the ground control points of some locations within the city. The National Population Commission (NPC) data was also employed to acquire the demographic statistics. The result of the study shows that the built-up area had expanded from 47.35 km^2 (10.76%) in 1986 to 71.05 km^2 (16.14%) in 2000 and to 284.68 km^2 (64.68%) in 2021. This expansion in built-up area generates a decline in wetland, bare land, and forest land from 112.296 km^2 (25.51%), 61.369 km^2 (13.94%), and 160.152 km^2 (36.39%) in 1986 to 72.468 km^2 (16.47%), 86.486 km^2 (19.65%), and 136.853 km^2 (31.09%) in 2000, and to 42.810 km^2 (9.73%), 10.858 km^2 (13.94%), and 40.8384 km^2 (9.28%) in 2021. The findings of the study are important because they give the government information on how quickly the study area is expanding, allowing it to adopt an appropriate planning strategy. In conclusion, the study demonstrate that remote sensing and GIS techniques can be utilized to successfully monitor the environment on a regular basis in order to investigate urban sprawl and inform better decision-making.

KEYWORDS

Land-Use Change, Greater Port Harcourt, Remote Sensing, Supervised Classification, Urban Sprawl

1. INTRODUCTION

Major cities in developing countries are experiencing urban sprawl, or the uncontrolled rise of a city's population (Balakeristanian and Md. Said, 2012). Many of these cities in developing countries, especially in Asia, as well as those in Africa, experience population explosion basically due to high birth rate and rural-urban migration, as people tend to move into cities mainly due to push factors (availability of job opportunities, basic amenities, and improved infrastructures) (Tahir et al., 2013). According to UN-Habitat, "urbanization" is the process of towns and cities expanding and developing, which results in a steady increase in the urban population and a decline in the rural population (UN-Habitat, 2006). It is the transition from rural to urban centers and the process by which a significant number of people live in a limited region (Katyanbo and Ngigi, 2017).

A characteristic of urbanization is the rise and extension of built-up regions as a result of the growing urban population (Guan et al., 2018). Urban sprawl frequently occurs incoherently and quickly spreads beyond the boundaries of major cities (Triantakonstantis and Mountrakis, 2012). Sprawl occurs either linearly along highways or radially around established cities (Wang et al., 2012). Various techniques could be used to analyze sprawl patterns. This mapping technique gives a "snapshot" of where urban sprawl is taking place, assisting in the identification of the resources that have been influenced and in making predictions about their anticipated future orientations and patterns (Hu et al., 2017). Other issues reliant on sprawl mapping and research include its effects on agricultural land use as well as other land uses such as industrial, residential, commercial, and institutional (Sisodai et al., 2014).

Documentation have revealed that in the year 1950, the world had 86 cities with a documented population of over a million people (Liu and Mason, 2013). Today, more than 400 cities exist, and by 2030, it's predicted that the number may rise to 600. Going by these figures, it is found that cities have really taken in about two-thirds of the increase in global population since 1950, and they are currently adding one million infants and migrants to that total each week (Lu et al., 2013). In Africa, approximately 1.3 billion people are anticipated to reside in urban areas by 2050, compared to the 0.35 billion who do so presently (United Nations, 2014). In Sub-Saharan Africa, urban population density was

Quick Response Code	Access this article online	
	Website: www.earthsciencesmalaysia.com	DOI: 10.26480/esmy.01.2023.36.42

Cite The Article: Chukwubueze Onwuzuligbo, Uzoma Chinenye Okeke, Onah Emmanuel Udochukwu, Iyam Ubi Effiom, John-Uri Kikpoye (2023). Modelling Urban Sprawl of The Greater Port Harcourt City Using Remote Sensing and Geographic Information System Techniques. *Earth Sciences Malaysia, 7(1): 36-42.*

found to rise from 27% in 1990 to 37% in 2014 and is expected to reach 55% in 2050. In contrast to the 0.3% change rate experienced by wealthy nations and the 1.7 change which is seen by the least developed governments, Sub-Saharan African is revealed to experience an average yearly change rate of 1.4% between 2010 and 2015 (United Nations, 2014).

Between 2010 and 2015, the percentage of people living in cities increased at a pace of 0.3% in developed nations and 1.2$ in developing nations, including 0.8% in South Africa. Africa and with Asia experiencing unprecedented urban population expansion at a higher rate. In Sub-Sahara Africa, informal settlements account for roughly 90% of urbanization, which is primarily accompanied by environmental degradation, poverty, unemployment, crumbling infrastructure, and unchecked informal settlement growth (United Nations, 2015). In Nigeria, suburban sprawl is featured as a haphazard housing growth, with the majority of buildings built without adequate planning and in fragmented layouts. It comprises of impromptu housing constructions on land that is owed by individuals, who sells their land in small, private plots, typically on the outskirts of cities. Shaw and reported that in Nigeria, built-up areas are peri-urban areas, and with the exurban regions outside of the suburbs (Shaw and Das, 2018; Wu and Zhang, 2012). According to reports by the United Nations, India, China, and Nigeria will together be responsible for 35% of the anticipated increase in the global urban population between 2018 and 2050 (United Nations, 2015). India is expected to have 416 million more urban residents by 2050, followed by China with 255 million and Nigeria with 189 million.

Remote Sensing and GIS are effective tools for gathering information that is helpful for monitoring urban areas (Shi et al., 2014). It has the ability to deliver information that was previously only available to specialized units to planners and decision-makers at competitive cost, opening up new ways for monitoring the dynamics of rapidly expanding settlements as opposed to the conventional methods, which are costly and time consuming. GIS enables the observation, visualization, monitoring, and forecasting of changes in land use (United Nations, 2014). Land use maps are produced using multispectral, multi-resolution, and multi-temporal data that can be exquisite using space or airborne sensors through remotely sensed data. In recent times, many researchers have applied remote sensing and GIS tools to study urban sprawl in different parts of the world. Researchers such as Magidi and Ahmed identified the spatio-temporal aspects of urban sprawl in the city of Tshwane from 1984 to 2015 using the supervised maximum likelihood classification and post-classification change detection approaches combined with Landsat data (Magidi and Ahmed, 2018).

Their findings, as evidenced by the categorized maps, demonstrate that urban sprawl has significantly increased over the past 31 years of the study period. A group researchers used maximum likelihood classification and post-classification change detection in conjunction with Landsat data to analyze the urban growth and change dynamics in Lagos, Nigeria, from 1990 to 2020 (Koko et al., 2020). Their research showed that the city's built-up area had significantly increased, but its vegetation cover, water volume, and bare land had decreased. A group researchers used supervised classification with a maximum likelihood classifier to collect spatial and temporal data from Landsat 5 TM, 7 (ETM +), and 8 (OLI/TIRS) images in order to explore land-use/land-cover change detection and urban growth in Gazipur district, Bangladesh, from 1990 to 2020 (Arifeen et al., 2021). The outcome demonstrates that there was a significant increase in urbanization over the study period, with the built-up area increasing by roughly a factor of five (18 to 104 km^2). A group reserchers used medium resolution satellite data from Landsat TM and ETM + from four dates (1986, 1991, 2002, and 2011) to study and examine the causes of urban sprawl in Akure in order to create a user-friendly geospatial database for tracking urban sprawl (Usman et al., 2018). The findings revealed that the built-up area in Akure increased during the study period. The study aim to model and map for urban sprawl in the Greater Port Harcourt city with Remote Sensing and Geographic Information System (GIS) tools.

2. Description of The Study Area

The Greater Port Harcourt (GPH) is found between Latitudes 4^{0}45'N and 4^{0}55'N and Longitudes 6^{0}55'E and 7^{0}05'E, at about 12 meters above mean sea level (Figure 1). The city is located in Rivers State, in the Nigerian Niger Delta at the River Bonny's mouth. Between the Bonny River and the Amadi Creek, Port Harcourt is roughly 25 kilometers from the Atlantic Ocean. Administratively speaking, GPH is an amalgamation of eight nearby villages in Port Harcourt. Before the creation of the Greater Port Harcourt law, Port Harcourt city was divided into three local governments, including the Obio-Akpo, and Okrika districts. Due to the recently constructed urban Master plan, the GPH city currently encompasses the administrative regions of Ikwerre, Oyigbo, Ogu-bolo, Etche, and Eleme (Ikechukwu, 2015). According to the Greater Port Harcourt Master Plan, the region will have a total population of 2,637,285 people by the year 2020, up from 1,884,570 at the time of the plan's inception in 2008. This means that the city must develop accommodations for an extra 700,000 people in addition to de-deifying the city and providing space for it. The city's predicted population growth over successive intervals is as follows:

2015	2.2 million
2020	2.6 million
2025	3 million
2030	3.4 million

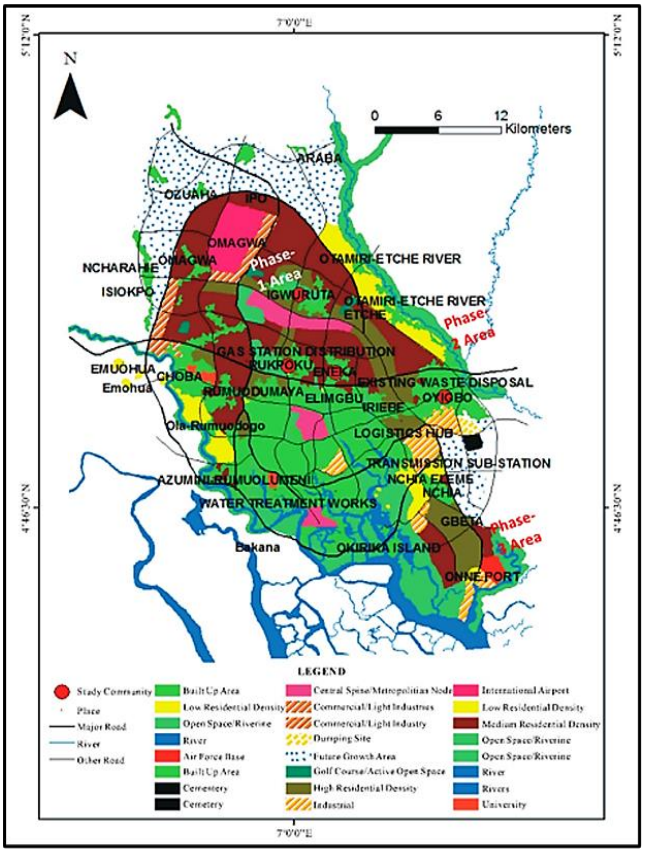

Figure 1: A map of the Greater Port Harcourt (GPH) Master Plan that depicts the location of the phases I, II and III (Ikechukwu, 2015)

3. Methodology

3.1 Sources of Data

In order to examine the urban sprawl of the Greater Port Harcourt city, three cloud-free Landsat images that were readily available from the GLCF throughout the dry season were used. Landsat 5 TM from 1986, Landsat 7 ETM+ from 2000, and Landsat 8 OLI/TIRS from 2021 were used (Table 1). A low-resolution image is one with a resolution of 30 meters, such as Landsat. The Geographic Position System (GPS) was used during field visits to collect the ground control points of some locations within the study area. To get the demographic statistics for the study area, the national Population Commission (NPC) data was employed. To obtain the plates, Google earth was used. Figure 2 shows the various stages of the image classification analysis for the study.

Table 1: Data Set Used in The Study

S/N	Data type	Year of Acquisition	Path	Row	Resolution	Source
1	Landsat 5 TM	1986	188	057	30 m	GLCF
2	Landsat 7 ETM+	2000	188	057	30 m	GLCF
3	Landsat 8OLI/TIRS	2021	188	057	30 m	GLCF

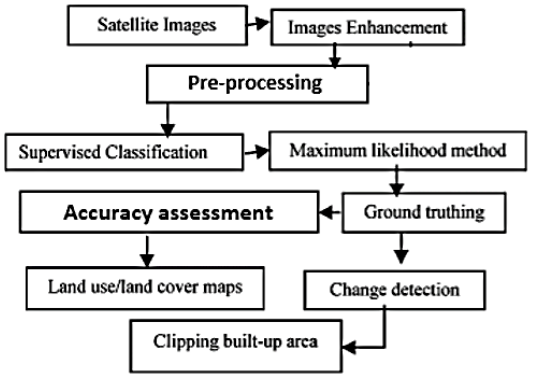

Figure 2: Image classification steps

3.2 Image Pre-Processing

In the study, Erdas Imagine 9.2 and ArcGIS 10.1 software were used to geo-reference the acquired Landsat images. The images were co-registered with the Universal Transverse Mercator (UTM) of 32N co-ordinate zone in the World Geodetic System (WGS 1984). Pre-processing actions, such as Image extraction, rectification, enhancement and image restoration were observed on the satellite image. Band combination and False colour composite (FCC) were observed in the study's satellite data before over laying the study area shape file and then sub-setting.

3.3 Image Classification

In the study, a post-classification method was performed in order to identify changes in the LULC classes at various epochs. Erdas Imagine 9.2 software was used to perform the pixel-based classification. The maximum, likelihood classifier was used to achieve supervised classification, which had involved recognizing pixels with similar spectral characteristics. Through classification, it was possible to determine the spectral signature of various features by using the signature in conjunction with the classifier tool of the Erdas Imagine.

3.4 Development of Classification Scheme

Following the prior understanding of the study area, a simplified classification scheme was created for the study. The LULC classification scheme proposed by Anderson, (1976) was modified, and then adopted for this study. The classification scheme adopted were built-up areas, bare land, vegetation, water bodies, and agricultural land (Table 2).

Table 2: Classification Scheme Adopted for The Study (Modified From Anderson, 1976).

Land use classes	Description
Built-up	Area of land used for residential, transportation, and communication
Bare land	Lands with exposed soil, that are without any vegetation
Vegetation	Terrain dominated by grasses, bushes, and plants
Water bodies	Area that are submerged under water, such as lakes, rivers, and dams.
Agriculture	Farmland, irrigation zones, and other spatially cultivated areas

3.5 Accuracy Assessment

Following the selection of pixels throughout the study region, ground truthing was conducted, and the acquired information was compared with the classified map. A good assessment of the accuracy of the entire map was provided by the number of random pixels that were verified and the proportion of accurate pixels (Enoh et al., 2022). Error matrix is often associated with accuracy assessment. Error matrix allows one to compare the pixels of a classified image with the pixels of a reference image for the study classes. Entries that are diagonally represented are considered to be correctly classified, while those that are non-diagonally are either error of omission (non-diagonal column entries) or error of commission (non-diagonal row entries) (Enoh et al., 2022).

3.6 Built-Up Extraction and Data Analysis

In order to understand the dynamic changes in urban sprawl in the research area, the built-up areas of the three epochs were derived from the categorized images. The built-up regions were retrieved from the image classification, which was used as an indicators to gauge urban sprawl. For each of the study years, the area of the resulting LULC types was evaluated in kilometers in order to ascertain the rate of change and compare the outcomes. In remote sensing, percentage change is a technique that is frequently employed to detect shifts in the different forms of land use. In order to discover the percentage change and trend between 1986 and 2000, as well as 2000 and 2021, it was helpful to compare the information on land use and land cover. The relationship is shown as follows (I):

Percentage change (Trend) = (observed change/sum of change) x 100 (I)

3.7 The Cellular Automata Model

A tool for prediction is the Cellular Automata Model (CA-Markov). It combines the Markov chain and cell automata analysis ideas (Singh et al., 2017). A dynamic process that is depicted in both time and space is the cellular automata model. It is laid out as follows:

$S\,(t+1) = f\,((S_t), N)$

S represents the finite groups of cells at time (t, t + 1), N represents the cell neighborhood, and f represents the local space rule.

4. Data Analysis and Results

4.1 Spatial Extent of LULC Classification

The spatial extent of the LULC classes of the study area in 1986, 2000, and 2021 is represented in Table 3. This study identified six types of LULC classes as wet land, built-up areas, forest land, water bodies, agricultural, and bare land.

As shown in Table 3, built-up changed from 47.356 km² (10.76%) in 1986 to 71.053 km² (16.14%) in 2000, and to 284.68 km² (64.68%) in 2021. This progressive change in built-up area is in agreement with the study of Ade and Afolabi (2013). Agricultural land, which was 14.802 km² (3.36%) in 1986, changed to 46.188 km² (10.49%) in 2000, and then decreased to 36.221 km² (8.23%) in 2021. These changes in agricultural and may be linked to changes in the built-up areas. Forest land was 160.152 km² (36.39%) in 1986, 136.853 km² (31.09%) in 2000, and 40.838 km² (9.28%) in 2021. In 1986, the bare surface was 61.369 km² (13.94%), 86.486 km² (19.65%) in 2000, and 10.858 km² (13.94%) in 2021. This might be linked to the conversion of bare surfaces to built-up areas. Wetland was 112.296 km² (25.51%) in 1986, 72.468 km² (16.47) in 2000, and 42.810 km² (9.73) in 2021. This could be due to transitions from wet land to built-up areas and bare surfaces. In 1986, the water surface changed from 44.154 km² (10.03%) to 27.081 km² (6.15%) in 2000, and to 23.723 km² (5.79%) in 2021. This change in water bodies could be due to the transition from water bodies to bare land especially during the dry season. It may also be attributed to sand filling. Table 4 shows the spatial extent of the LULC classes in the study. Table 5–7 shows the confusion matrix table for the study from 1986 to 2021.

Table 3: Spatial extent of LULC classes.

Study years / Land use	1986		2000		2021	
	Area-km²	Area-%	Area-km²	Area-%	Area-km²	Area-%
Wet land	112.2960	25.51	72.4683	16.47	42.8106	9.73
Built-up area	47.3562	10.76	71.0532	16.14	284.679	64.68
Forest land	160.1523	36.39	136.8531	31.09	40.8384	9.28
Water bodies	44.1540	10.03	27.0810	6.15	23.7231	5.39
Agricultural land	14.8023	3.36	46.1880	10.49	36.2213	8.23
Bare land	61.3692	13.94	86.4864	19.65	10.8576	13.94
Total	**440.1300**	**100**	**440.1300**	**100**	**440.1300**	**100**

Table 4: Magnitude of Change in the LULC Classes			
Land use of the study area	**Extend of urban sprawl between 1986 and 2000**	**Extend of urban sprawl between 1986 and 2021**	**Extend of urban sprawl between 2000 and 2021**
Wet land	- 39.8277	- 69.4854	- 29.6577
Built-up area	23.6970	237.3228	213.6258
Forest land	- 23.2992	- 119.3239	- 96.0147
Water bodies	- 17.0730	- 20.4309	- 3.3579
Agricultural land	31.3857	21.419	- 9.9667
Bare land	25.1172	- 50.5116	- 75.6288

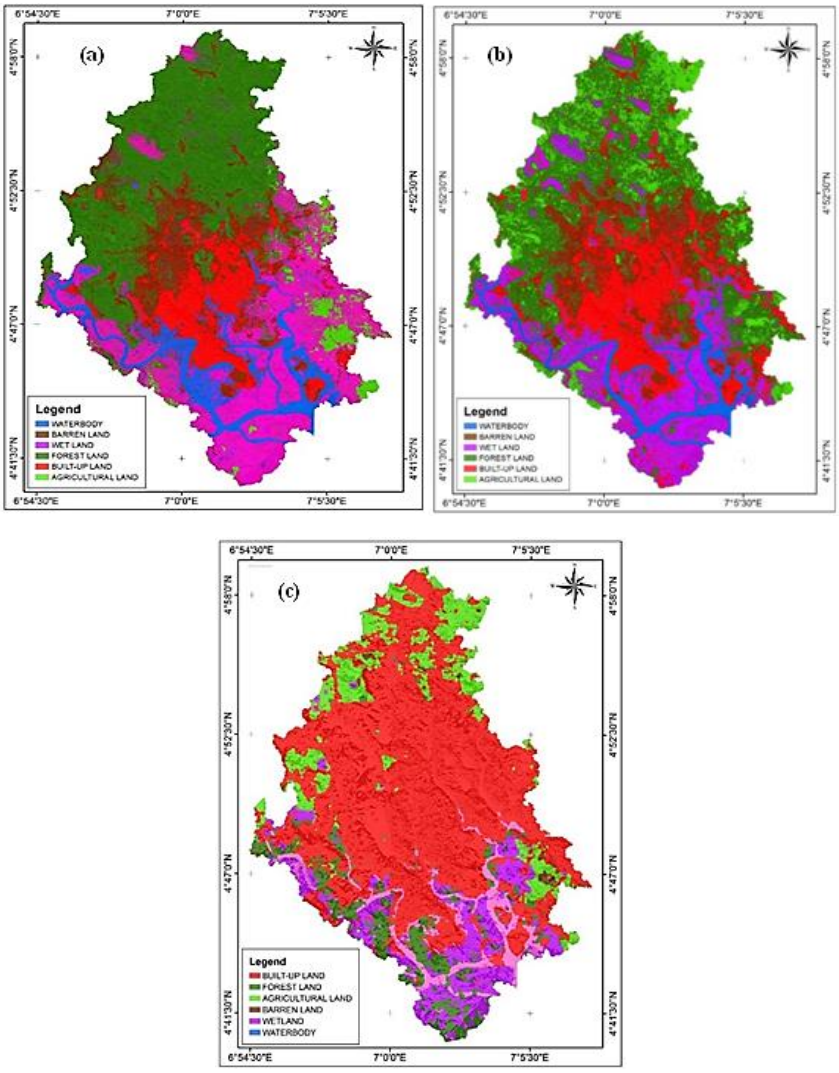

Figure 3: (a)–(c). Spatial extent of LULC classes of the study area (1986–2021)

Table 5: Confusion matrix of the estimated total number of pixels (1986)							
1986	**Ground**						**No. of classified pixels**
	Wet land	**Build-up**	**Forest land**	**Water bodies**	**Agricultural land**	**Bare land**	
Wet land	46	2	1	0	1	0	50
Built-up area	0	43	0	0	5	2	50
Forest land	1	1	44	1	3	0	50
Water bodies	1	0	1	48	0	0	50
Agricultural land	1	0	2	1	46	0	50
Bare land	0	0	3	1	0	46	50
No. of ground truth pixels	49	46	51	51	55	48	300

Overall Landsat classification accuracy

Correctly classified samples = 46 + 43 + 44 + 48 + 46 + 46 = 273

Total number of samples = 273

Overall accuracy = 273/300 = 0.91 (or 91%)

Table 6: Confusion Matrix of the Estimated Total Number of Pixels (2000)

2021	Ground						No. of classified pixels
	Wet land	Build-up	Forest land	Water bodies	Agricultural land	Bare land	
Wet land	46	0	1	1	1	1	50
Built-up area	0	43	0	3	2	2	50
Forest land	1	1	44	1	2	1	50
Water bodies	1	0	2	45	0	2	50
Agricultural land	1	2	2	0	42	3	50
Bare land	0	2	1	0	3	44	50
No. of ground truth pixels	49	48	50	50	50	53	300

Overall Landsat classification accuracy

Correctly classified samples = 43 + 45 + 44 + 47 + 44 + 44 = 264

Total number of samples = 264

Overall accuracy = 264/300 = 0.88 (or 88%)

Table 7: Confusion Matrix of The Estimated Total Number of Pixels (2021)

2021	Ground						No. of classified pixels
	Wet land	Build-up	Forest land	Water bodies	Agricultural land	Bare land	
Wet land	47	1	1	1	0	0	50
Built-up area	1	44	0	0	3	2	50
Forest land	1	2	41	1	2	3	50
Water bodies	1	1	1	47	0	0	50
Agricultural land	0	2	2	1	44	1	50
Bare land	0	4	1	0	1	44	50
No. of ground truth pixels	50	54	46	50	48	52	300

Overall Landsat classification accuracy

Correctly classified samples = 47 + 44 + 41 + 47 + 44 + 44 = 270

Total number of samples = 267

Overall accuracy = 267/300 = 0.89 (or 89%)

4.2 Analysis of Urban Sprawl in the Study Area

By careful evaluating how built-up areas in the study area developed, and grew, urban sprawl was assessed. The quantitative quality of urban land usage in 1986, 2000, and 2021 is shown in Table 8.

Figure 4 (a) is a map that depicts the spatial extent of the built-up area in 1986. This development highlights the clustered and radii forms of sprawl. Figure 4 (b) shows the spatial extent of the built-up areas during the year 2000. If we compare Figures 4 (a) and (b), we see that the map in Figure 4 (b) shows more concentrated clusters and leapfrog settlement. This is an indication of urban sprawl in the study area over time. Figure 4 (c) shows the spatial extent of the built-up area in 2021. Here, the settlements are mostly in clustered, radii, and leapfrog form.

Table 8: The Extent of Urban Sprawl in 1986, 2000, and 2021.

Year	Rate of urban growth (km²)	(%)
1986	47.3562	12.34
2000	71.0532	18.36
2021	268.6028	69.40
Total	387.0122	100

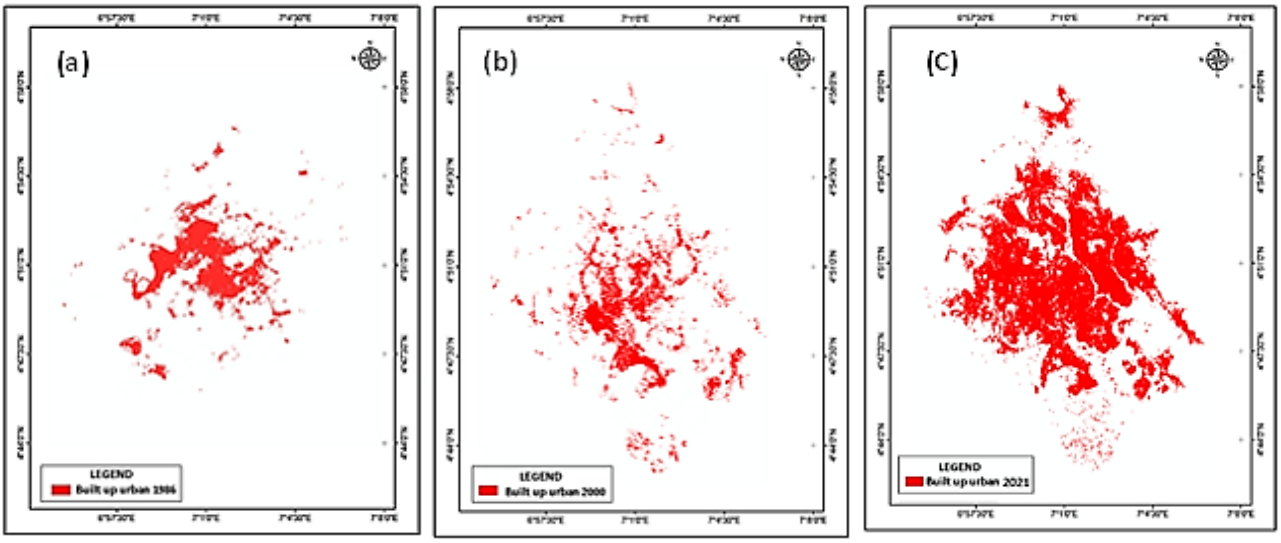

Figure 4: (a)–(c) The spatial extent of built-up area in the Greater Port Harcourt city (1986–2021)

Figure 5 is a map that shows the spread of settlement in an overlay form (1986–2021). By visualization, we see from the map legend that the yellow pixels depicts built-up area during 1986, while the blue and green pixels highlight the built-up areas during 2000, and 2021 study years.

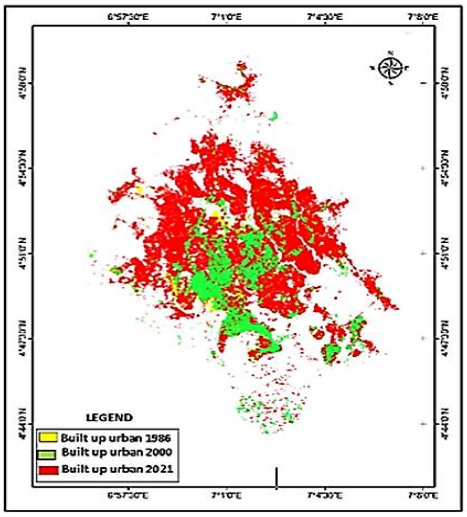

Figure 5: The spatial extent of urban sprawl in the study area (1986–2021)

4.3 Urban Sprawl Projection Analysis (2030)

Table 9 shows the projected LULC classes for the study area for 2030.

Table 9: Projected LULC Values for 2030

LULC classes	Area (in km²)	Area (in %)
Wet land	38.1543	8.669
Built-up area	305.4387	69.397
Forest land	32.6740	7.424
Water bodies	21.5873	4.905
Agricultural land	26.6208	6.048
Bare land	15.6549	3.557
Total	**440.1300**	**100**

Figure 6 is a map that shows the LULC classification for the study area for 2030. This map was produced with the Markov chain application in the Idrisi Selva software. By visualization, we see from the map legend that the built-up area is shown in red, and is far more clustered than the LULC built-up of 2021. We also note that the built-up area, which is expanding, is encroaching into other land-cover areas. Owing to the analysis, land cover such as forests, water bodies, and agricultural land has been threatened in the study area, and is fast disappearing.

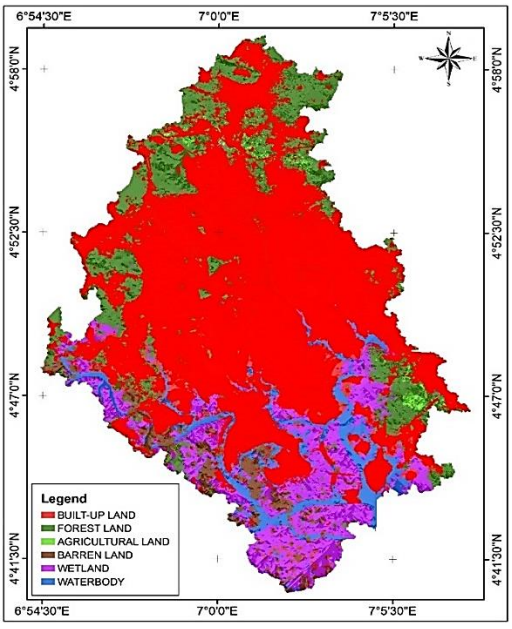

Figure 6: Projected LULC map for 2030

Table 9 shows that the population of the study area has been gradually growing over time. The following social-economic implications could manifest in the study region by 2030, if this scenario is maintained:

i. Communal conflict may develop between farmers and herdsmen, due to the scarcity of land for both cultivation and cattle grazing.

ii. Residents living in the study area may be experiencing an increase in crime primarily due to rising unemployment. There may be an upsurge in crime including kidnapping, robberies, and pickpocketing.

iii. There will be a lot of traffic congestion in the study area. This is accurate, as there may be more transportation facilities compared to the limited available highways, given that the population is predicted to grow.

iv. By 2030, the study area's social infrastructure-such as electricity, schools, and pipe-borne water will be underdeveloped and overburdened.

v. The land may be under a lot of pressure as new residents, recreation areas, schools, and other structures will be constructed to meet the population's continued growth.

vi. By 2030, the study area will experience an increase in erosion issues, flooding, loss of arable land, and the destruction of open areas.

5. Conclusions

This study shows that remote sensing and GIS tools can be used to analyze urban sprawl. The findings of this study showed that built-up areas had witness a positive change during the study years while other study classes (wetland, forest land, and water bodies) had declined throughout the study period. Agricultural and bare land had increased and decreased during the course of study. The positive change in the built-up area may have been linked to high birth rate, and rural urban migration, as more people move to the study area, due to push factors. In recent times, the state government's goal to reinstate Port Harcourt city to its original status as the state capital by demolishing all types of illegal structures inside its borders has also contributed to the area's recent population growth. The study shows that the study area have been experiencing a significant increase in population over the thirty five (35) years from 1986 to 2021. This can be deduced by the fact that the land area occupied by built-up areas, which include residential, industrial, commercial, and institutional is growing. This change in built-up area has an impact on other LULC classes like wetland, bare land, and forest land.

References

Ade, M.A., Afolabi, Y.D., 2013. Monitoring urban sprawl in the Federal Capital Territory of Nigeria using Remote Sensing and GIS techniques. Ethiopian Journal of Environmental Studies and management, 4, Pp. 82–95.

Anderson, J.R., 1976. A land use and land cover classification scheme for use with remote Sensing.

Arifeen, H.M., Phoungthong, K., Mostafaeipour, A., Yuanggyai, N., Yuangyai, C, Techato, K, Jutidamrongphan, W., 2021. Determine the Land-Use Land-Cover Changes, Urban Expansion and their driving factors for sustainable development in Gazipur Bangladesh. Atmosphere, 12, Pp. 1353.

Balakeristanian, M.I., Md Said M.A., 2012. Land use Land cover change detection using remote sensing application for land sustainability. American Institute of Physics, 1482, Pp. 425–430.

Enoh, M.A., Njoku, R.E., Okeke, U.C., 2022. Modeling and mapping the spatial-temporal changes in land use and land cover in Lagos: A dynamics for building a sustainable urban city. Advances in Space Research, In Press, Corrected Proof.

Hu, X., Zhou, W., Qian, Y., Yu, W., 2017. Urban expansion and local land cover change both significantly contribute to urban warming, but their relative important changes over time. Landscape Ecology, 32, Pp. 768–780.

Ikechukwu, E.E., 2015. The socio-economic impact of the Greater Port Harcourt Development project on the residents of the affected areas. Open Journal of Social Science, 3, Pp. 82.

Koko, A.F., Yue, W., Abubakar, G.A., Hamed, R., Alabsi, A.A.N., 2021. Analyzing urban growth and land cover changes scenario in

Lagos, Nigeria using multi-temporal remote sensing data and GIS to mitigate flooding. Geomatics, Natural Hazards and Risk, 12 (1), Pp. 631–652

Liu J.G., Mason P.J., 2013. Essentail Image Processing and GIS for Remote Sensing. John Wiley $ Sons, New Jersey, USA.

Lu, C., Wu, Y., Shen, Q., Wang, H., 2013. Driving force of urban growth and regional planning: A case study of China's Guangdong Province. Habitat International, 40, Pp. 35–41.

Magidi, J., Ahmed, F., 2018. Assessing urban sprawl using remote sensing and landscape metrics: A case study of City of Tshwane, South Africa (1984-2015). The Egyptian Journal of Remote Sensing and Space Sciences, Pp. 335–346

Shaw, R., Das, A., 2018. Identifying peri-urban growth in small and medium towns using GIS and remote sensing technique: a case study of English Bazar urban agglomeration, West Bengal, India. Egypt Journal of Remote Sensing and Space Sciences, 21 (2), Pp. 159–172.

Shi, J., Wn, J., Paul, A., Jiao, L., Gong, M., 2014. Change detection in synthetic aperture radar images based on fuzzy active contour models and genetic algorithms. Mathematical Problems in Engineering, Volume 2014 | Article ID 870936 | https://doi.org/10.1155/2014/870936.

Singh, P., Kikon, N., Verma, P., 2017. Impact of land use change and urbanization on urban heat island in Lucknow city. Central India. A remote sensing-based estimate. Sustain. Cities Soc. 32, Pp. 100-114.

Sisodai, P., Tiwari, V., Kumar, A., 2014. Analysis of supervised maximum likelihood classification for remote sensing image. International conference on recent advances and innovations in engineering, ICRAIE.

Tahir, M., Imam, E., Hussain, T., 2013. Evaluation of land use/land cover changes in Mekelle city, Ethiopia using remote sensing and GIS. Computational ecology and Software, 3, Pp. 9–16.

Triantakonstantis, D., Mountrakis, 2012. Urban growth prediction: A review of computational models and human perceptions. Journal of Geographic Information System, 4, Pp. 555–587.

United Nations, 2014. World Urbanization Prospects" The 2014 revision, New York.

Usman, V.A., Makinde, E.O., Salami, A.T., 2018. Geospatial Assessment of the impact of urban sprawl in Akure, Southwestern Nigeria. Journal of Geoscience and Environmental Protection, 6, Pp. 123–140.

Wang, S.Q., Zheng, X.Q., Zang, X.B., 2012. Accuracy assessment of land use change simulation based on Markov-cellular automata model. Procedia Environmental Science, 13, Pp. 1238–1245.

Wu, K.Y., Zhang, H., 2012. Land use dynamics, built-up land expansion patterns, and driving forces analysis of the fast-growing Hangzhou metropolitan area, Eastern China (1978–2008). Applied geography, 34, Pp. 137–145.